Coulomb Luttinger liquid

D. W. Wang,[1] A. J. Millis,[2] and S. Das Sarma[1]

[1]*Department of Physics, University of Maryland, College Park, Maryland 20742-4111*
[2]*Center for Materials Theory and Department of Physics and Astronomy, Rutgers University, New Brunswick, New Jersey 08554*

Accurate expressions, valid in experimentally relevant regimes, are presented for the effect of a long-ranged Coulomb interaction on the low-energy properties (momentum distribution function, density of states, electron spectral function, and $4k_F$ correlation function) of one-dimensional electron systems. The importance of plasmon dispersion (as opposed to exponent) effects in the spectral function is demonstrated.

The low-energy behavior of one-dimensional (1D) electron systems is known not to be consistent with Fermi liquid theory.[1] However, the theoretically well-established[2] and extensively studied[3] Luttinger liquid (LL) model of one-dimensional physics[4] is, strictly speaking, not applicable to electronically conducting one-dimensional systems such as quantum wires (QWR's),[5] carbon nanotubes,[6] organic conductors,[7] and doped chain or ladder compounds,[8] because the electrons in these compounds interact via the Coulomb force, which is long ranged, whereas the standard Luttinger model assumes a short-ranged interaction. The long range of the Coulomb interaction leads to a scale dependence of the Luttinger exponents and velocities,[9] which have been studied by several authors[9,10] on the assumption that it is well approximated by its leading ($\ln^{1/2}$) divergence. As we show, this approximation is not accurate in any physically relevant regime. One exception is a very interesting recent renormalization group treatment[11] which found an effective exponent very similar to ours but did not discuss the implications for physical quantities. Some numerical results have also appeared,[12] but a general understanding of the experimental implications of the Coulomb interaction is lacking.

In the present paper we use direct analytical and numerical evaluation of the relevant bosonization expressions to determine the momentum distribution function, tunneling density of states, and spectral function for 1D electron systems interacting via the physically relevant Coulomb interaction at zero temperature. We define an important but previously overlooked energy scale, present an accurate expression for the scale-dependent exponent, show how the scale-dependent velocity affects the spectral function, and qualitatively discuss the $4k_F$ correlation function. Our results should apply directly to 1D QWR's (Ref. 5) and nanotubes.[6]

We consider a 1D electron system with a noninteracting dispersion ε_p which we linearize near the Fermi point, defining a bare velocity v_F. We here assume that the only important interaction is the Coulomb interaction in the forward scattering channel and neglect umklapp scattering and other interactions. This is a good approximation for QWR and nanotube systems. [For organic and doped spin chain materials a modification, discussed below Eq. (2), is needed.] The Hamiltonian is (here we do not write the spin index explicitly)

$$H = \sum_{r,p} v_F(p - rp_F)c_{r,p}^\dagger c_{r,p} + \frac{1}{L}\sum_{r,q} V_c(q)[\rho_r(q)\rho_r(-q)$$
$$+ \rho_r(q)\rho_{-r}(-q)], \tag{1}$$

where $c_{r,p}^\dagger$ is the electron creation operator and $\rho_r(q)$ is the density operator describing density fluctuations at momentum q and branch $r = \pm 1$ for the right (left) movers. For 1D systems $V_c(q) \rightarrow \ln(1/q)$ as $q \rightarrow 0$ and becomes $1/q$ for q larger than some scale q_0 set by the geometry and the wave function size. A reasonable approximate form, which we will use in our subsequent analysis, is

$$V_c(q) = \frac{\pi v_F V_0}{2}\ln\left[\frac{q_0 + q}{q}\right], \tag{2}$$

where V_0 is a dimensionless measure of the interaction strength and q_0^{-1} is the length scale parameter. V_0 and q_0 are system-dependent factors. For a cylindrical quantum wire of radius a, $V_0 = 4e^2/\pi\varepsilon_0 v_F$ and $q_0 \sim 2.5/a$, where e is the electron charge and ε_0 is the background dielectric constant, about 10 for GaAs. These values give the correct long-wavelength limit and are within 10% of the correct $1/q$ coefficient at large momentum. In carbon nanotubes V_0 is of the same form as in QWR's but $\varepsilon_0 \sim 1.4^6$ and $q_0 \sim 2.97/R$, where R is the radius of the tube. For organics or doped spin chains, additional short-ranged exchange interactions may be important. The usual arguments[2] show that these interactions lead, at low energies, to an additive constant term in $V_c(q)$.

Equation (1) may be bosonized as usual[2,3]; the charge excitations are plasmons with dispersion $\omega_q = qv_q$, and velocity $v_q \equiv v_F\sqrt{1 + 2V_c(q)/\pi v_F}$ is

$$v_q = v_F\sqrt{1 + V_0\ln\left[\frac{q_0 + q}{q}\right]}. \tag{3}$$

(Note that we have $\lim_{q\rightarrow\infty}\omega_q \sim qv_F + V_0q_0/2 \neq qv_F$ for the Coulomb interaction.) The electron Green function $G_r(x,t) \equiv \langle\psi_r(xt)\psi_r^\dagger(00)\rangle$ is

$$G_r(x,t) = \lim_{\epsilon\rightarrow 0}\frac{e^{irk_F x}}{2\pi}\frac{i\exp[-\Phi_r(x,t)]}{x - rv_Ft + i\epsilon}, \tag{4}$$

where the phase function $\Phi_r(x,t)$ is

$$\Phi_r(x,t) = \frac{1}{2}\int_0^\infty \frac{dp}{p} e^{-\epsilon p}(e^{ip(x-rv_Ft)} - e^{ip(x-rv_pt)})$$
$$+ 2\sinh^2(\theta_p)[1-\cos(px)e^{-irpv_pt}]. \quad (5)$$

The exponent parameter θ_p is defined by

$$e^{-2\theta_q} = \sqrt{1 + V_0\ln\left(\frac{q_0+q}{q}\right)} \sim \sqrt{V_0}\ln^{1/2}\left(\frac{q_s}{q}\right), \quad (6)$$

where $q_s \equiv q_0 e^{1/V_0}$ and the last approximation is good at long wavelengths, $q \ll q_0$.

We now use Eqs. (4)–(6) to study electronic quantities. We begin with the momentum distribution function

$$n_r(\delta p) = \frac{-i}{2\pi}\int_{-\infty}^\infty dx \frac{e^{-i\delta px}}{rx-i\epsilon}\exp[-\Phi_r(x,0)], \quad (7)$$

where $\delta p \equiv p - rk_F$. In a noninteracting Fermi gas, $n_r(\delta p) = \theta(-r\delta p)$. For a short-ranged LL, the generally accepted result[13] is that in the vicinity of the Fermi momentum, $0.5 - n_r(\delta p) \sim \text{sgn}(r\delta p) \times \{C_1|\delta p| + C_2|\delta p|^\gamma\}$ with γ a LL exponent and C_1 and C_2 two constants. The first term is the noncritical background coming from high energies, while the second (critical) term comes from low energies where LL physics is important. For the long-ranged interacting model we now consider, attention to the singularity structure of the noninteracting electron Green function leads to (let $\delta p > 0$ and $r = +1$)

$$n(\delta p) = \frac{1}{2} - \frac{1}{\pi}\int_0^\infty \frac{dx}{x}\sin(\delta px)\exp[-\Phi(x,0)]$$
$$= \frac{1}{2} + C_1'\delta p + C_2'\left(\frac{\delta p}{q_0}\right)^{\gamma_q(\delta p)} + \text{higher orders}, \quad (8)$$

where again the nonsingular C_1' term is from the integration over small x, while the singular C_2' term comes from integration over large x and is a weak function of $\ln^{1/2}(1/\delta p)$. The scale dependent exponent $\gamma_q(\delta p)$ is found to be

$$\gamma_q(q) \sim \frac{1}{2}\left(\frac{1}{3}e^{-2\theta_q} + e^{2\theta_q} - 1\right)$$
$$\sim \frac{\sqrt{V_0}}{6}\ln^{1/2}\left(\frac{q_s}{q}\right) + \frac{\ln^{-1/2}(q_s/q)}{2\sqrt{V_0}} - \frac{1}{2}. \quad (9)$$

Figure 1 shows results obtained by numerically evaluating Eq. (8) for typical QWR parameters. An enhanced curvature near the Fermi momentum is evident. The inset of Fig. 1 shows the logarithmic derivative $\alpha_q(p) \equiv d\ln|n(p) - 1/2|/d\ln(p)$, which shows that for small δp the behavior may be described in terms of a slowly changing effective exponent. We note that $\alpha_q(p)$ is always less than 1, because when the scale-dependent exponent $\gamma_q(p)$ of Eq. (9) is greater than 1, the background term dominates.

We now turn to the tunneling density of states,
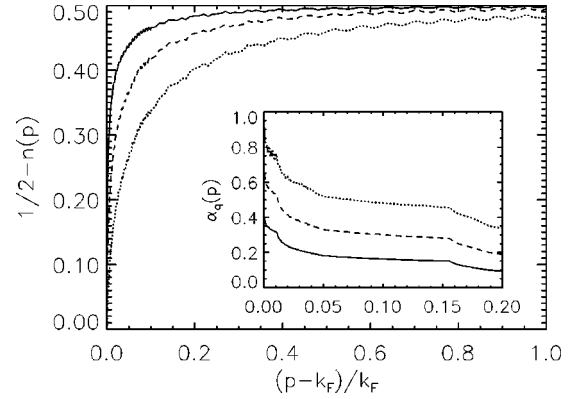
FIG. 1. Calculated momentum distribution function $n(p)$ with respect to momentum $p - k_F$ for a realistic QWR system of $a = 70$ nm. Solid, dashed, and dotted lines are results for three different interaction strengths $V_0 = 1.21$, 2.42, and 4.84, respectively, where $V_0 = 1.21$ is for electron density 0.65×10^6 cm^{-1} and $\varepsilon_0 = 12.7$ (Ref. 5). Inset: the effective exponent (around k_F) obtained by taking the logarithmic derivative of the numerical $n(p)$ for $|p - k_F| < 0.2k_F$.

$$N(\omega) = \frac{1}{2\pi}\sum_r \int_{-\infty}^\infty dt\, e^{i\omega t}[G_r(0,t) + G_r(0,-t)], \quad (10)$$

for ω measured from the chemical potential.

We first show that $N(\omega)$ vanishes faster than any power of ω as $\omega \to 0$. We observe that if $V_c(p) \neq 0$, G vanishes faster than any power of t as $t \to \infty$.[9] Therefore the integral obtained by taking any number of ω derivatives of $N(\omega)$ is absolutely convergent at long times, and may be evaluated straightforwardly by contour methods even at $\omega = 0$.[14] We further note that $G_r(0,t)$ has no singularities in the lower (upper) half plane for $r = +1$ (-1); thus by deforming the contours appropriately we find that $d^n N(\omega)/d\omega^n|_{\omega=0} = 0$ for any n. This argument does not apply to $n(p)$ because of the different analytic structure of the x dependence. Thus the noncritical contributions which obscured the behavior of $n(p)$ do not occur in $N(\omega)$. By evaluating Eq. (10) we obtain

$$N(\omega) \propto \left(\frac{\omega}{\omega_s}\right)^{\gamma_\omega(\omega)}, \quad (11)$$

where the scale-dependent density of states exponent $\gamma_\omega(\omega)$ is

$$\gamma_\omega(\omega) \sim \frac{\sqrt{V_0}}{6}\ln^{1/2}\left(\frac{\omega_s}{\omega}\right) + \frac{\ln^{-1/2}(\omega_s/\omega)}{2\sqrt{V_0}} - \frac{1}{2}, \quad (12)$$

the same form as that of Eq. (9) with q_s replaced by a characteristic energy scale ω_s. From Eqs. (3) and (6) we expect $\omega_s = A q_s v_F\sqrt{V_0}$ with the numerical constant A determined by subleading corrections to the asymptotic analysis of Eq. (5). Here A may in principle have a weak scale and system-parameter dependence, but our numerical results show that for a wide range of energies ($10^{-3} < \omega/E_F < 0.1$) and interactions ($1 < V_0 < 5$) it is very well approximated by the con-
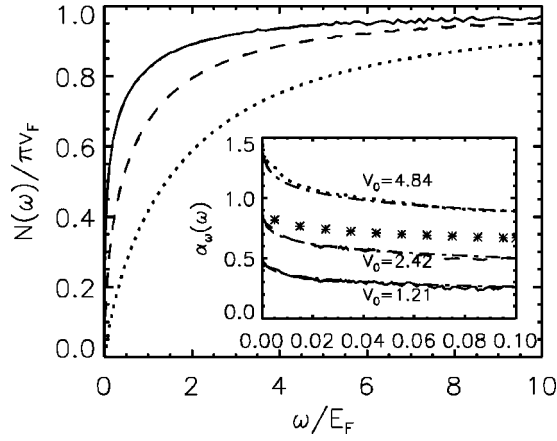
FIG. 2. Calculated density of states, $N(\omega)$, with respect to energy ω for the same system as Fig. 1. Different line styles represent different interaction strengths as indicated. The inset is the effective exponent α_ω obtained by taking the logarithmic derivative of $N(\omega)$. The numerically calculated curves are well fitted by the analytical expression (dash-dotted lines) of the exponent from Eq. (13) at the corresponding V_0's and $\omega_s = 20 q_s v_F \sqrt{V_0}$. The stars are the first-order term of Eq. (13) only, for $V_0 = 1.21$, showing that the widely used leading logarithm approximation leads to factor of 2 errors.

stant value $A = 20$. Figure 2 shows the results of a numerical calculation of $N(\omega)$ from Eq. (10) for three different interaction strengths; the inset compares the numerically calculated effective exponent $\alpha_\omega(\omega) \equiv d \ln[N(\omega)]/d \ln(\omega)$, with the analytical result obtained from Eqs. (11) and (12):

$$\alpha_\omega(\omega) = \frac{\sqrt{V_0}}{4} \ln^{1/2}\left(\frac{\omega_s}{\omega}\right) + \frac{\ln^{-1/2}(\omega_s/\omega)}{4\sqrt{V_0}} - \frac{1}{2}. \quad (13)$$

One sees that the fit is very good (the small differences appearing at $\omega/E_f \sim 0.01$ arise from noise in the numerical calculation).

The two crucial energy scales defined by $N(\omega)$ are ω_s and ω_* at which $\alpha_\omega(\omega_*) = 1$, corresponding to $\omega_* \sim \omega_s e^{-34/V_0} \ll \omega_s$. In the high-energy region $\omega > \omega_s$, one has essentially noninteracting behavior. For $\omega_* < \omega < \omega_s$, one has a LL with a scale-dependent exponent. For $\omega < \omega_*$, $\alpha_\omega > 1$ and $N(\omega)$ is concave upwards at small ω, suggesting a ''pseudogap'' in the electronic density of states. For most real QWR systems, V_0 is about 1–5 depending on ε_0 and v_F, and thus ω_* is typically many orders of magnitude smaller than ω_s. In our calculation, using QWR parameters from Ref. 5, we have $\omega_s \sim 100$ meV and $\omega_* \sim 10^{-4}$ meV. For extremely small $\omega \ll \omega_*$, Eq. (13) gives $\alpha_\omega \sim (\sqrt{V_0}/4)\ln^{1/2}(\omega_s/\omega)$, an approximate form used earlier in the literature.[9,10] However, as seen from the inset of Fig. 2, the leading logarithmic divergence is so weak that in all physically relevant regimes the other two terms in Eq. (12) are needed for quantitative accuracy. On the other hand, the constant (scale-independent) exponent used in Ref. 6 for nanotubes is also not an adequate approximation for the small energy region ($\omega < 0.05 E_F$) ei-

ther. We therefore propose Eqs. (9) and (12) as widely applicable fitting formulas for the effective exponents in the Coulomb Luttinger liquid.

The scale-dependent exponent also appears in the single-particle spectral function $\rho(q,\omega) = (1/2\pi)[G(q,\omega) + G(-q,-\omega)]$; however, the scale-dependent velocity in Eq. (5) is more important. To introduce our results, we briefly summarize known results for a short-ranged repulsive interaction in the spinless LL model.[13] At fixed q, one defines three ω ranges: (i) $\rho(q,\omega) = 0$ for $|\omega| < \omega_q$ (energy-momentum conservation), (ii) power-law singularities as $|\omega| \to \omega_q^+$, and (iii) an exponential decay at scales larger than the Luttinger cutoff. For the long-ranged Coulomb interaction, $\rho(q,\omega) = 0$ for $|\omega| < \omega_q$ due to the energy-momentum conservation, but the behavior in both regions (ii) and (iii) is strongly modified. For $|\omega| > \omega_s$ [region (iii)], $\rho(q,\omega) \sim \exp[-|\omega|/E_c(\omega)]$ with a scale-dependent cutoff

$$E_c(\omega) = \frac{q_0 v_F V_0}{4} \ln\left(\frac{a|\omega|}{v_F}\right), \quad (14)$$

because of the slow $(1/q)$ decay of the Coulomb interaction in the large momentum region [Eq. (5)].

Near threshold ($\omega_q < |\omega| \ll \omega_s$) there are two effects: the scale dependence of the effective Luttinger exponent and the curvature of the plasmon dispersion, which prevents the different boson modes from adding coherently. Thus as one decreases ω towards ω_q (consider $\omega > 0$ part only) one obtains first a divergence $\delta\omega^{\gamma_\omega(\delta\omega)-1}$ (here $\delta\omega \equiv \omega - \omega_q$). This divergence is cut off by curvature effects at a scale $\omega_c(q) \equiv \text{Max}_{p<q}(\omega_p - p\omega_q/q) \approx (1/4)q v_F \sqrt{V_0}\ln^{-1/2}(q_s/q)$, the difference between the exact dispersion and a linear approximation. We find that for q larger than $q_* \sim A q_s e^{-75/V_0}$ [at which $\gamma_\omega(\omega_c(q_*)) = 1$] the curvature effect is more important in cutting off the divergence, whereas for $q < q_*$ the effective exponent is more important. As $\delta\omega \to 0^+$ the spectral function decreases rapidly, ultimately vanishing faster than any power of $\delta\omega$ due to the increase of the effective exponent. Thus the generic behavior is a spectral function which increases rapidly as ω is increased above threshold ω_q, goes through a maximum at $\omega_{peak} = \omega_q + \Delta\omega$ with $\Delta\omega$ set by the larger of ω_* and $\omega_c(q)$, and then decreases exponentially with a scale-dependent cutoff $E_c(\omega)$ for $\omega > \omega_{peak}$. The suppressed spectral weight in the near-threshold region is compensated by the slower decay at high energies, preserving the sum rule $\int \rho(q,\omega) d\omega = 1$. In Fig. 3 we show the results of direct numerical evaluation of the electron spectral function for the Coulomb Luttinger liquid (solid lines) and for a short-ranged-interaction (regular) Luttinger liquid with exponent $\alpha = 0.2$, approximately equal to the effective exponent of the Coulomb case at $\omega = 0.3 E_F$ (dashed lines). Note that the partition theory techniques used in Ref. 15 to simplify the evaluation for the short-ranged case do not work in the Coulomb case. The shift of the peak away from the threshold is evident.

Finally, we briefly discuss the ''Wigner crystal'' correlation. Schultz[9] observed that at long enough length scales the logarithm arising from the long-ranged Coulomb interaction
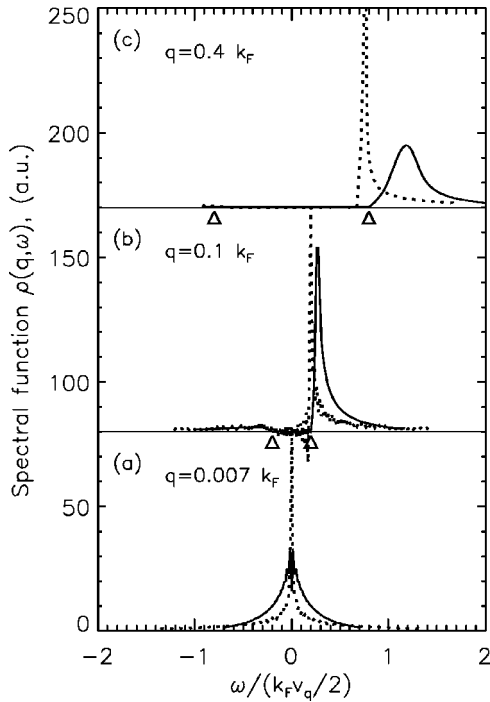
FIG. 3. Calculated electron spectral function $\rho(q,\omega)$ for different momenta q as indicated in the figure. Solid lines are from the Coulomb interacting system (parameters are the same as Fig. 1 with $V_0=1.21$) while dotted lines are from the short-ranged interacting system with the approximate effective exponent $\alpha=0.2$. The two triangles in (b) and (c) indicate the threshold $\omega=\pm\omega_q$. The ripple of the spectral function curves is the numerical error.

causes the $4k_F$ component of the density-density correlation to decay more slowly than x^{-4K_ρ} and also more slowly than the $2k_F$ component, leaving a state best interpreted as a Wigner crystal. Using the notation of this paper, we obtain, for the $4k_F$ term in the structure factor,

$$S_{4k_F}(\delta p) \sim \left(\frac{q_s}{\delta p}\right)^{1-8V_0^{-1/2}\ln^{-1/2}(q_s/\delta p)}, \qquad (15)$$

where $\delta p \equiv |p-4k_F|$. Therefore we expect to see the $4k_F$ divergence when $\sqrt{V_0}\ln^{1/2}(q_s/\delta p)>8$ or $\delta p < q_s e^{-64/V_0}$, or in terms of temperature at $T<T_{w.x}=\omega_s e^{-64/V_0}$, which is sensitive to the electron density and experimental geometry, but is in general far too small to be experimentally relevant and is also much less than the scale ω_* at which $N(\omega)$ develops a pseudogap.

Before concluding we critically discuss the various approximations made in our theory in the following. (i) We have used an approximate form of the 1D Coulomb interaction through the simple model defined by Eq. (2). This approximation is qualitatively correct, but the cutoff length scale q_0^{-1} is system dependent and may not be known in general. (ii) We have neglected umklapp and other possible (e.g., impurity-induced) large-q corrections in our calculation primarily because such corrections do not arise in semiconductor quantum wire systems which are of main interest to us. If umklapp processes are important, that could change our results. We believe that our theory is the correct leading order theory for the Coulomb Luttinger liquid and the neglected corrections are small.

In conclusion, we have presented a systematic theoretical analysis of the low-energy properties of electron systems subject to long-ranged Coulomb interactions, including a reliable estimate of the scale-dependent Luttinger parameter and apparently the first calculation of Coulomb effects on the spectral function and values for the (unfortunately extremely low) scales at which the divergent behavior associated with the Coulomb interaction becomes manifest.

[1] A. Luther and V.J. Emery, Phys. Rev. Lett. **33**, 589 (1974); I.E. Dzyaloshinkii and A.I. Larkin, Sov. Phys. JETP **38**, 202 (1974).

[2] F.D.M. Haldane, J. Phys. C **14**, 2585 (1981).

[3] J. Voit, Rep. Prog. Phys. **58**, 977 (1995).

[4] The low-energy behavior of spinful fermions with SU(2) symmetry should be described by a Wess-Zumino-Witten model leading to small corrections usually neglected and irrelevant here. For details, see I. Affleck, in *Fields, Strings and Critical Phenomena*, Les Houches Session XLIX 1998, edited by E. Brezin and J. Zinn Justin (Elsevier, Vancouver, 1989).

[5] A.R. Goñi et al., Phys. Rev. Lett. **67**, 3298 (1991).; See also O.M. Auslaender et al., *ibid.* **84**, 1764 (2000).

[6] M. Bockrath et al., Nature (London) **397**, 598 (1999); C. Kane et al., Phys. Rev. Lett. **79**, 5086 (1997); R. Egger and A.O. Gogolin, *ibid.* **79**, 5082 (1997).

[7] F. Zwick et al., Phys. Rev. Lett. **81**, 2974 (1998); D. Jerome, J. Phys. IV **10**, 69 (2000).

[8] E. Dagotto and T.M. Rice, Science **271**, 618 (1996).

[9] H.J. Schulz, Phys. Rev. Lett. **71**, 1864 (1993).

[10] M. Fabrizio et al., Phys. Rev. Lett. **72**, 2235 (1994); M. Franco and L. Brey, *ibid.* **77**, 1358 (1996); A. Iucci and C. Naón, Phys. Rev. B **61**, 15 530 (2000).

[11] S. Bellucci and J. González, Eur. Phys. J. B **18**, 3 (2000).

[12] G. Fano et al., Phys. Rev. B **60**, 15 654 (1999); S. Capponi et al., *ibid.* **61**, 13 410 (2000).

[13] J. Voit, J. Phys.: Condens. Matter **5**, 8305 (1993).

[14] Y. Suzumura, Prog. Theor. Phys. **63**, 5 (1980).

[15] K. Schönhammer and V. Meden, Phys. Rev. B **47**, 16 205 (1993); U. Zülicke and A.H. MacDonald, Phys. Rev. B **54**, R8349 (1996).